Transverse surface-induced polarization at the interface between a chiral nematic liquid crystal and a substrate

Ishtiaque M. Syed and Charles Rosenblatt*
Department of Physics, Case Western Reserve University, Cleveland, Ohio 44106-7079
(Received 25 November 2002; published 17 April 2003)

A chiral nematic liquid crystal that is tilted by an angle θ_i with respect to a substrate is subjected to an ac electric field at frequency ω applied parallel to the substrate. The nematic director is found to oscillate azimuthally about the normal to the liquid crystal–substrate interface at frequency ω, indicating that a nonzero polarization perpendicular to the molecular tilt plane exists at the interface. The interfacial polarization, anchoring strength coefficient, and bulk viscosity are obtained by measurements of the oscillation amplitude as a function of ω.

DOI: 10.1103/PhysRevE.67.041707 PACS number(s): 61.30.Gd

In 1975, Meyer *et al.* demonstrated the existence of ferroelectricity for chiral molecules in the smectic-*C* phase, also known as the smectic-*C** phase [1]. Owing to the system's C_2 symmetry, a spontaneous electric polarization of magnitude P_0 lies perpendicular to the tilt plane of the molecules and parallel to the smectic layers. In simple mean-field theory, the polarization is proportional to the polar tilt angle θ, although deviations have been observed due to higher-order couplings between P_0 and θ [2–6]. Nearly 12 years ago, the possibility that such a polarization may exist in a *nematic* phase composed of chiral molecules that are tilted at a substrate interface was examined [7]. Owing to C_1 symmetry at the interface, one would expect to find a ''transverse polarization'' perpendicular to the molecular tilt plane (analogous to that in the smectic-*C** phase), as well as a component of polarization normal to the interface. In order to examine the transverse polarization, we applied a strong magnetic field H to a homeotropically aligned cell, inducing a bend Fréedericksz transition at a threshold field H_{th}. Since the surface anchoring strength is finite for $H \gg H_{th}$, a polar tilt θ_i is obtained at the interface. An ac electric field E at angular frequency ω was then applied perpendicular to the polarization vector and parallel to the interface, causing the director to oscillate azimuthally by an angle φ_i (at frequency ω). It was found that the oscillation amplitude φ_i is proportional to the applied electric field, demonstrating the existence of a transverse surface-induced polarization. Nevertheless, because it was necessary to use a magnetic field to generate a significant nonzero polar tilt at the surface, the polar angle $\theta(z)$ by necessity varied with position z throughout the bulk. This precluded proper analysis of both the tilt angle dependence and the dynamic aspects of this effect.

Very recently, we showed [8] that it is possible to treat a particular polyimide, which under ordinary circumstances promotes homeotropic alignment, so that the liquid crystal exhibits a large ''pretilt'' angle θ_i. By extended baking of the polyimide SE1211 (Nissan Chemicals) and subsequent rubbing, we found that θ_i may be controlled up to $\approx 45°$ for the liquid crystal pentylcyanobiphenyl. We suggested that the extra baking enhances the degree of imidization of the polymer and that the unidirectional rubbing extends the now more rigid backbone. The director adopts an equilibrium angle θ_i that is determined by the relative interactions with the planar-promoting backbone and the homeotropic-promoting side chains. Although the pretilt angle characteristics depend on both the polyimide treatment and the nature of the liquid crystal, we have found that the chiral liquid crystalline mixture SCE12 (Merck) can exhibit large values of θ_i. Thus, it now becomes possible to examine the transverse surface-induced polarization effect in the *absence* of a magnetic field, facilitating quantitive studies of the temperature, polar tilt angle, and dynamical behavior. In this paper we report on both the quasistatic and dynamic behavior of this effect, and extract polarization, azimuthal anchoring strength coefficient, and viscosity information from the dynamic data.

An indium-tin-oxide coated glass slide was etched chemically to leave two parallel conducting strips approximately $l = 2$ mm apart. This facilitated application of an electric field $E = 2V/\pi l$ in the plane of the cell [7], where V is the potential difference between the electrodes. Both this slide and an ordinary microscope slide were cleaned and then spin coated with the polyimide SE1211 and baked at 200° for 1 h to ensure homeotropic alignment. Both slides were then rubbed with a cotton cloth using a rubbing machine and placed together, separated by Mylar spacers, in an antiparallel configuration. This configuration of the preferred orientation directions of the two polyimide surfaces ensures that the liquid crystal molecules have the same orientation at both surfaces, as shown in Fig. 1, and that $\theta(z) = \theta_i$ throughout the cell. The thickness at the middle of the cell was measured by an interferometry technique and found to be $d = (3.4 \pm 0.1)$ μm. The cell was then placed in an oven that was temperature controlled to ≈ 10 mK and filled with the chiral mixture SCE12 in its isotropic phase. The phase sequence for SCE12 is isotropic 119°C–nematic–82°C –smectic-*A*–66°C–smectic-*C**. On cooling into the nematic phase at temperature T_{NI}, the material exhibited the classic fingerprint texture of a chiral nematic. However, the pitch of the mixture is designed to become large (>100 μm) near the nematic–smectic-*A* phase transition temperature T_{NA}. We found that within 14°C of T_{NA}, the pitch became sufficiently

*Author to whom correspondence should be addressed. Email address: cxr@po.cwru.edu

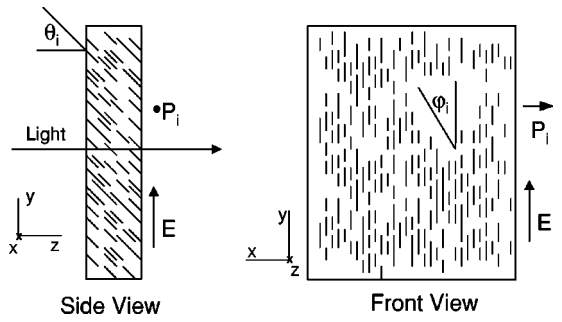

FIG. 1. Schematic view of cell. Incident optical polarization is at an angle of $\pi/8$ with respect to the y axis in the xy plane. Immediately after cell, analyzer is oriented at an angle $\pi/2$ with respect to polarizer. Side view shows that the director is spatially uniform in the absence of an electric field. The polarization P_i resides at the two interfaces. Application of an electric field causes a torque on the polarization and an azimuthal rotation of the molecules. Front view shows the azimuthal orientation passing through $\varphi=0$ as the electric field oscillates with time.

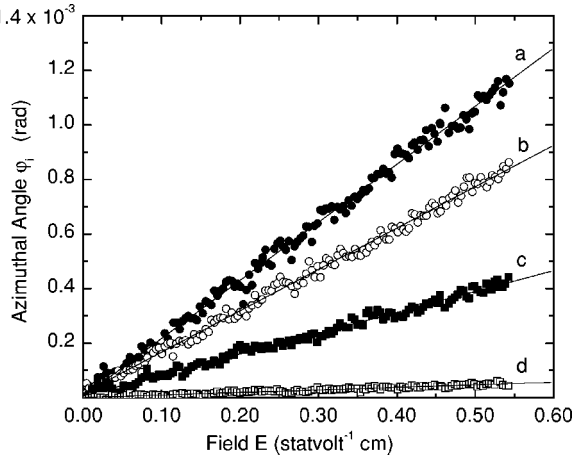

FIG. 2. Amplitude of azimuthal rotation φ_i vs applied field E for four different temperatures: (a) 83°C, (b) 87°C, (c) 91°C, and (d) 95°C.

large as to unwind the helix, resulting in a surface-stabilized monodomain homeotropic texture [9].

The beam from a 5-mW He-Ne laser, focused to a spot size of ~ 80 μm midway between the electrodes, was incident on the sample. The beam was polarized at an angle of $\pi/8$ with respect to the rubbing direction in the classical ''electroclinic geometry'' [10]. After being recollimated by a second lens, the beam passed through an analyzer and into a photodiode detector. The output of the detector was fed into both a lock-in amplifier that was referenced to the driving frequency ω of the electric field, and a dc voltmeter. These measured the ac intensity I_{ac} at frequency ω and the dc intensity I_{dc}, respectively.

The electric polarization associated with the tilted chiral molecules at the two surfaces couples to the ac electric field, causing the director to oscillate azimuthally. The interior of the liquid crystal, which has zero net polarization, is driven elastically by the surface molecules and thereby oscillates with the field. To understand the optics, let us consider the Mauguin limit [11,12]–this is also known as ''adiabatic following'' and is the principle behind the twisted nematic display, in which the optical polarization rotates with the director twist. This limit requires $2\lambda/\Delta n(\theta_i) \ll$ helical pitch, where $\lambda=633$ nm is the wavelength of light, $\Delta n(\theta_i)\approx(n_e-n_o)\theta_i^2$ is the effective optical birefringence, and the effective helical pitch has a lower limit of $\pi d/\varphi_i$ [13], where φ_i is the azimuthal orientation at the interface. For extraordinary refractive index $n_e=1.638$ and ordinary index $n_o=1.481$, which were measured with an Abbe refractometer and are approximately constant over the temperature range of the experiment, and for $\theta_i \sim 0.1$ rad, we find $\Delta n \sim 0.0015$; thus $2\lambda/\Delta n(\theta_i) \sim 10^{-1}$ cm. Since the effective helical pitch >1 cm for $\varphi_i < 10^{-3}$ rad (see below), the system is in the Mauguin limit: The extraordinary and ordinary polarizations follow the director's azimuthal variation through the cell and emerge at the rear of the cell *as if* the azimuthal director orientation were spatially uniform throughout the cell. In fact, in the limit $\omega=0$ the azimuthal orientation *is* uniform throughout the cell. At higher frequencies, however, it is not uniform and the fact that we have adiabatic following of the light greatly simplifies the analysis of the dynamical behavior. Thus, as described above, for our ''electroclinic geometry'' we measure both I_{dc} and I_{ac} (at frequency ω); the azimuthal orientation φ_i of the director at the interface is given by $\varphi_i = I_{ac}/4I_{dc}$ [10]. Although $\varphi(z) \leqslant \varphi_i$ in the interior of the cell, especially at higher driving frequencies, the Mauguin limit for the optics ensures that the quantity $I_{ac}/4I_{dc}$ corresponds to φ_i.

At a given temperature, an applied electric field at frequency $\omega=57\ \mathrm{s}^{-1}$ (corresponding to 9 Hz) was ramped from 0 to 0.55 statvolts cm^{-1} rms at a rate of 7.6×10^{-4} statvolts $\mathrm{cm}^{-1}\mathrm{sec}^{-1}$ and the intensities I_{ac} and I_{dc} were recorded. We shall see below that this frequency is sufficiently low such that the response of the liquid crystal is quasi-dc, wherein the azimuthal angle $\varphi(z)$ throughout the cell is approximately uniform and equal to φ_i. Measurements were made as a function of temperature in the nematic phase and the deduced azimuthal angles $\varphi_i(T)$ vs E are shown in Fig. 2 at four representative temperatures.

In Fig. 3, we plot the slope of φ_i vs E data and see that the quantity $d\varphi_i/dE$ decreases with decreasing temperature. This behavior is due to the fact that the polar pretilt angle θ_i is temperature dependent, and goes to zero near the nematic–smectic-A phase transition temperature T_{NA}. (A detailed study of the behavior of $\theta_i(T)$, which is a result of the interplay among anchoring associated with *two* easy axes and surface-induced smectic order, is reported elsewhere [14]). In order to determine $\theta_i(T)$, the analyzer and polarizer were adjusted to make an angle of 45° with respect to the rubbing direction. A Babinet-Soleil compensator was introduced between the sample and the analyzer and was used to measure the optical retardation α of the cell as a function of temperature. We then determine $\theta_i(T)$ from the relationship $\Delta n(\theta_i)=\lambda\alpha/2\pi d = n_o n_e (n_o^2\sin^2\theta_i + n_e^2\cos^2\theta_i)^{-1/2} - n_o$. Deduced values of $\theta_i(T)$ are shown in Fig. 4.

To examine the frequency response, intensity data were collected at $T=89$°C. The electric-field-induced azimuthal

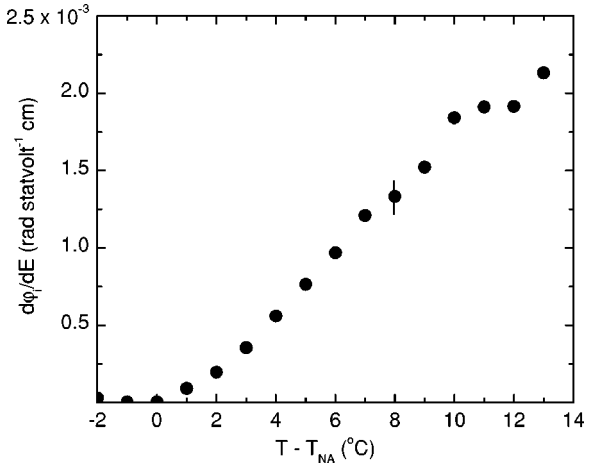

FIG. 3. $d\varphi_i/dE$ vs reduced temperature. Typical error bar is shown.

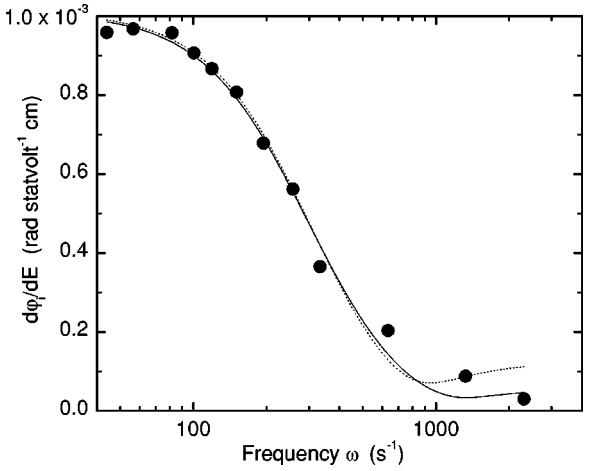

FIG. 5. $d\varphi_i/dE$ vs frequency ω at $T=89°$C. Solid line corresponds to a least-squares three-parameter fit of the data to Eq. (3); dashed line corresponds to the predicted behavior using a different set of three parameters (see text).

angle $\varphi_i = I_{ac}/4I_{dc}$ was measured as a function of field at a given frequency, and the quantity $d\varphi_i/dE$ was extracted. In Fig. 5, we show $d\varphi_i/dE$ vs frequency.

To understand the results we note that the applied electric field couples primarily to the two interfacial regions [15], which in turn couple elastically to the bulk. The elastic free-energy density is given by $F_{el}=\frac{1}{2}k(d\varphi/dz)^2$, where $k=K_{22}\sin^2\theta$ and K_{22} is the usual twist elastic constant. Applying the Euler-Lagrange equation and introducing a viscosity η, we obtain the diffusion equation $\eta d\varphi/dt = kd^2\varphi/dz^2$ for the director orientation in the bulk. At a frequency ω, the magnitude of φ is given by

$$\varphi = \left|\mathrm{Re}\{[A\exp(-\sqrt{i\omega\eta/k}z)+B\exp(\sqrt{i\omega\eta/k}z)]e^{i\omega t}\}\right|. \tag{1}$$

Taking the two interfaces at $z=d/2$ and $z=-d/2$, the coefficients A and B are determined by the condition that $d\varphi(z=0,t)/dz=0$ and by the torque balance equation

$$-kd\varphi_i/dz + W_i\varphi_i = P_iE \tag{2}$$

at either interface i. The quantity P_i is the polarization of the *interfacial layer* and has dimensions of charge per unit length. The quantity W_i corresponds to the azimuthal anchoring strength coefficient and has dimensions of energy per unit area. Assuming that there is a preferred axis $\varphi_i^{pref}=0$ for azimuthal orientation—this corresponds to the rubbing direction—the energy cost associated with an azimuthal orientation φ_i that differs from φ_i^{pref} to the lowest order is $\frac{1}{2}W_i(\varphi_i-\varphi_i^{pref})^2$. From the general solution [Eq. (1)], the torque balance equation, and the condition of symmetry at the center of the cell, it is easy to show that the magnitude of $d\varphi_i/dE$ is

$$\frac{d\varphi_i}{dE} = \left|\mathrm{Re}\left\{\frac{P_ie^{i\omega t}}{W_i-\sqrt{i\omega\eta k}\tanh(d\sqrt{i\omega\eta/k}/2)}\right\}\right|. \tag{3}$$

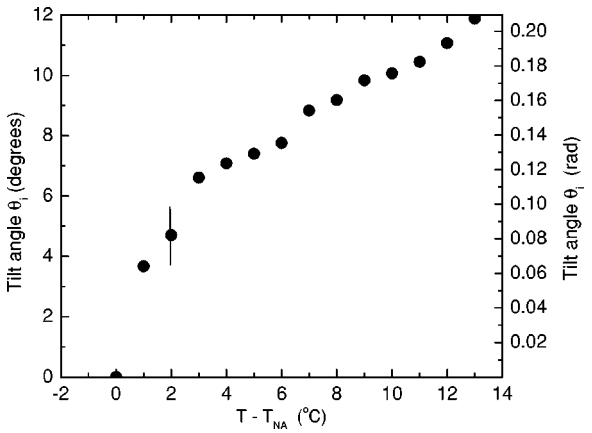

FIG. 4. Measured polar tilt angle θ_i vs reduced temperature.

At sufficiently low driving frequency $d\varphi_i/dE \approx P_i/W_i$. From Fig. 5 we see that the quasi-dc regime corresponds to $\omega \lesssim 100\ \mathrm{s}^{-1}$, justifying our use of $\omega = 57\ \mathrm{s}^{-1}$ for the quasi-dc data reported in Figs. 2 and 3. On symmetry grounds we now make the assumption that the anchoring strength coefficient $W_i \propto \theta_i^2$ for small θ_i. The dependence of polarization on tilt angle is more problematical, where a simple mean-field model predicts that $P_0 \propto \theta$ in the bulk smectic-C^* phase [1]. Assuming the behavior of the nematic at the interface mimics the behavior in a smectic-C^* layer, the quasi-dc limit $d\varphi_i/dE \approx P_i/W_i$ suggests that the quantity $\theta_i d\varphi_i/dE$ should be constant as a function of emperature, and thus as a function of θ_i Examination of Figs. 3 and 4 clearly shows that this is *not* the case. In fact, in Fig. 6 we plot the bulk polarization P_0 vs θ in the smectic-C^* phase, as extracted from the manufacturer's specifications for P_0 vs T and for θ vs T. It is obvious that the polarization is *not* linear in θ over the range shown. Modifications to the simple $P_0 \propto \theta$ relationship have been proposed [3,16,17] and generally involve a coupling term proportional to $P_0^2\theta^2$ in the free energy. Such a term would result in a polarization of the form $P_0 \propto \theta/(1-a\theta^2)$ in the smectic-C^* phase, where a is a constant. On fitting the manufacturer's P_0 vs θ data in Fig.

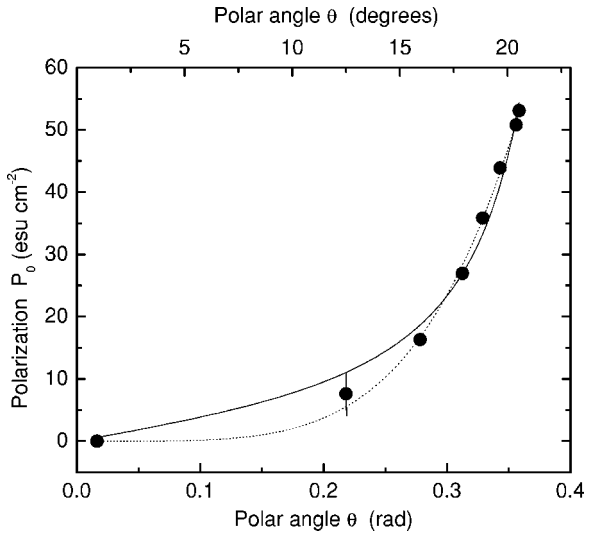

FIG. 6. Bulk polarization P_0 vs polar tilt angle θ in smectic-C^* phase of SCE12, extracted from manufacturer's specifications for P_0 vs T and θ vs T. Solid line represents fit to the form $P_0 \propto \theta/(1-a\theta^2)$ and dotted line to the form $P_0 \propto \theta^b$, where $b=4.5\pm0.2$.

(6) to this form, we find $a \sim (5.2\pm0.8)$ rad $^{-2}$ (solid line). If we were to apply this form for polarization to our quasi-dc data, Eq. 3 would suggest that the quantity $\theta_i(1-a\theta_i^2)d\varphi_i/dE$ would be independent of T in the quasi-dc limit. Again, this is not the case as $\theta_i(1-a\theta_i^2)d\varphi_i/dE$ varies considerably with temperature and even vanishes at T_{NA}. Thus the form $P_i \propto \theta_i/(1-a\theta_i^2)$ does not seem to apply at the interface. An attempt to fit the manufacturer's data for P_0 vs θ (Fig. 6) in the smectic-C^* phase to the *ad hoc* form $P_0 \propto \theta^b$ results in $b=4.5\pm0.2$ (dotted line). On applying this form to the interfacial polarization P_i, we find that the quantity $\theta_i^{2-b}d\varphi_i/dE$ $[=\theta_i^{-2.5}d\varphi_i/dE]$ is considerably more uniform with temperature (Fig. 7), at least compared to the previous two scaling forms. Thus, our data indicate that the surface polarization P_i in the nematic phase varies *very* rapidly with θ_i, which seems to differ from the behavior of the bulk polarization P_0 in the smectic-C^* phase. Indeed, the observed behavior may be derived from a temperature-dependent segregation of species that comprise the SCE12 mixture at the interface, and/or coupling between the two easy axes proposed as the mechanism that drives the director away from homeotropic orientation [14]. Although it is beyond the scope of this work, the behavior of P_i vs θ_i is clearly a fertile topic for future investigation.

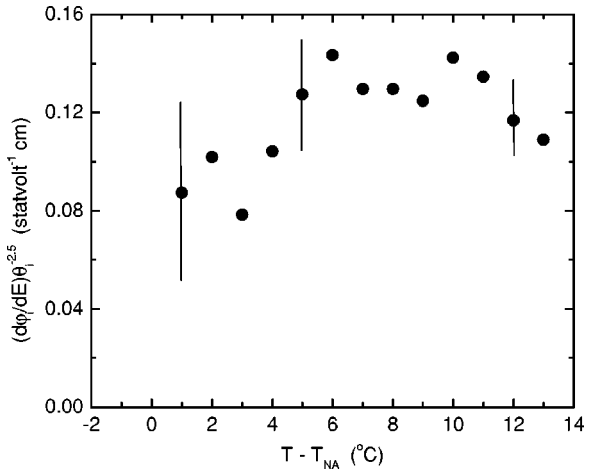

FIG. 7. $(d\varphi_i/dE)\theta_i^{-2.5}$ vs reduced temperature. Data indicate that the interfacial polarization P_i must vary very rapidly with θ_i, at least compared to the behavior in the bulk smectic-C^* phase.

As an aside, we note that measurements of $d\varphi_i/dE$ and of θ_i vs T were also made with the racemic version of this mixture, SCE12R. We found that on examining $d\varphi_i/dE$ at comparable polar tilt angles for the two materials, $d\varphi_i/dE$ for the racemic mixture was at least two orders of magnitude smaller than for the chiral material, and generally within the noise. This clearly demonstrates that the observed phenomenon is due to the chiral symmetry at the interface.

Let us now turn to the frequency-dependent results in Fig. 5. At higher frequencies, $d\varphi_i/dE$ becomes small because the interior of the cell is unable to follow, and exerts a restraining elastic force on the interfacial region. We used Eq. (3) with three free parameters–P_i, W_i, and η–to fit the data in Fig. 5, where $k=2\times10^{-8}$ dyn was held fixed. This is a reasonable value for the projection of the twist elastic constant K_{22} at $T=89°$C ($\sim$30 K into the nematic phase), where $\theta_i \approx 0.16$ rad. The resulting fitted parameters are the layer polarization $P_i=(1.1\pm0.5)\times10^{-8}$ esu cm^{-1}, the bulk viscosity $\eta=(2.4\pm1.1)\times10^{-4}$ P, and the azimuthal anchoring strength coefficient $W_i=(1.1\pm0.5)\times10^{-5}$ erg cm^{-2}; the fitted curve is shown by the solid line in Fig. 5. If we assume that the thickness of the interfacial region is approximately a molecular length ($\sim2\times10^{-7}$ cm), then the effective volumetric polarization would be ≈0.06 esu cm^{-2}. This is two orders of magnitude smaller than the corresponding polarization P_0 in the bulk smectic-C^* phase (cf. Fig. 6), indicating that the coupling of the molecular dipoles to the local environment is considerably weaker at the nematic-substrate interface as compared to a bulk smectic-C^* layer. There are several reasons for the weaker coupling. First, the degree of smectic order induced by the substrate is likely to be quite weak so far above T_{NA} [18], and this would tend to inhibit strong intermolecular correlations associated with a smectic layer. Moreover, the rubbed polyimide in which the backbone is partially elongated in the plane of the substrate [8,14] is rough on molecular length scales. Finally, the existence of two competing easy axes from the backbones and side chains—this is the likely cause of the macroscopic pretilt ($0 \leqslant \theta_i \leqslant \pi/2$) [14]—also may compete in biasing the dipole moment. The net result is a weaker coupling of the molecular dipoles to the local symmetry, and a reduced polarization P_i. Turning now to the viscosity, a simple scaling argument would suggest that $\eta=\eta_0\theta_i^2$ for small θ_i. On dividing the viscosity by the square of the polar tilt angle, we obtain an effective viscosity $\eta_0 \approx 0.01$ P. This is an eminently reasonable value, especially given the high temperature at which the measurements were performed. Last, we turn to the fitted azimuthal anchoring strength coefficient W_i. Again we would expect that $W_i=W_0\theta_i^2$ for small θ_i, where W_0 corresponds to the azimuthal anchoring strength

coefficient in the limit that $\theta_i = \pi/2$. From our fitted value of W_i, we find that $W_0 \approx 5 \times 10^{-4}$ erg cm^{-2}. This figure appears to be rather small, although reports exist of azimuthal anchoring strength coefficient values of the order of 10^{-3} erg cm^{-2} [19]; our result is not too much smaller than this. We do not have any immediate explanation for our small value of W_0, although the suggested existence of a pair of easy axes (planar and homeotropic) in part may be responsible.

For comparison purposes, the same sort of frequency-dependent measurements were performed at a higher temperaure, $T = 95°$C, where $\theta_i \approx 0.21$ rad. As expected from the larger polar tilt angle at this temperature, the fitted polarization $P_i = (2.5 \pm 1.0) \times 10^{-8}$ esu cm^{-1} was enhanced by a factor of ≈ 2 compared to the $T = 89°$C result. The anchoring strength coefficient $W_i = (1.3 \pm 0.5) \times 10^{-5}$ erg cm^{-2}, which should have been enhanced by more than 50%, in fact is only $\sim 15\%$ larger than at $T = 89°$C, although this discrepancy still is within the fitting uncertainty. The viscosity $\eta = (2.7 \pm 1.1) \times 10^{-4}$ P, which might be expected to exhibit Arrhenius behavior and decrease at higher temperatures, actually was found to increase by $\approx 15\%$. We feel that the Arrhenius behavior was more than compensated by the increased polar tilt at higher temperature, resulting in an increase in viscosity.

It is important to note that our data, when fitted to Eq. (3), admits other reasonable values for the parameters, especially if data at high frequencies are given less weight. For example, the dotted line in Fig. 5 shows the behavior of $d\varphi_i/dE$ at $T = 89°$C using the parameters $P_i = 2.3 \times 10^{-8}$ esu cm^{-1}, $\eta = 4.8 \times 10^{-4}$ P, and $W_i = 2.3 \times 10^{-5}$ erg cm^{-2}. First, notice that the ratio P_i/W_i is fixed by the low-frequency behavior of $d\varphi_i/dE$. Thus, scaling both P_i and W_i by the same factor leaves the low-frequency behavior unchanged. Similarly, the viscosity must increase by approximately the same factor in order to maintain the central part of the curve. The largest deviation from the first fit (solid line) occurs only in the high-frequency regime. Thus, we feel that our dynamical data fits are appropriate for obtaining magnitudes of P_i, W_i, and η, as well as demonstrating the phenomenon of interfacial polarization. However, we do not have sufficient confidence in the fits to discriminate between fitted parameters that may differ by factors of, e.g., 2.

The results presented in this paper demonstrate that a chiral nematic liquid crystal tilted at an interface exhibits a polarization component at the interface that is perpendicular to the tilt plane. Frequency-dependent data, moreover, facilitate a measurement of the magnitudes of the polarization, anchoring strength coefficient, and twist viscosity. The results raise a number of questions. How does the interfacial polarization scale with polar tilt angle θ_i, and why does P_i vs θ_i apparently differ from the behavior in the bulk smectic-C^* phase? Why is the interfacial polarization divided by the molecular length approximately two orders of magnitude smaller than the bulk polarization in the smectic-C^* phase? Why is the scaled anchoring strength coefficient (W_i/θ_i^2) apparently smaller—by about one order of magnitude—than typical values at a planar aligned substrate? The answers to these questions to a great extent depend on the microscopic orienting mechanism of the rubbed polyimide, and will be the subject of future investigations.

We thank Dr. Rolfe Petschek, Dr. Wen Bing, and Dr. Tatsutoshi Shioda for useful discussions. This work was supported by the National Science Foundation under Grant No. DMR-9982020, the U.S. Department of Energy's Office of Basic Energy Science under Grant No. DE-FG02-01ER45934, and by the Donors of the Petroleum Research Fund, administered by the American Chemical Society, under Grant No. 37736-AC7.

[1] R.B. Meyer, L. Liebert, L. Strzelecki, and P. Keller, J. Phys. (France) Lett. **36**, L69 (1975).
[2] C. Filipic, A. Levstik, I. Levstick, R. Blinc, B. Zeks, M. Glogarova, and T. Carlsson, Ferroelectrics **73**, 295 (1987).
[3] T. Carlsson, B. Zeks, A. Levstik, C. Filipic, I. Levstik, and R. Blinc, Phys. Rev. A **36**, 1484 (1987).
[4] J. Schacht, H. Baethge, F. Giesselmann, and P. Zugenmaier, J. Mater. Chem. **8**, 603 (1998).
[5] F. Gießelmann and P. Zugenmaier, Phys. Rev. E **52**, 1762 (1995).
[6] S. Dumrongattana and C.C. Huang, Phys. Rev. Lett. **56**, 464 (1986).
[7] S. Tripathi, M.-H. Lu, E.M. Terentjev, R.G. Petschek, and C. Rosenblatt, Phys. Rev. Lett. **67**, 3400 (1991).
[8] G.P. Sinha, B. Wen, and C. Rosenblatt, Appl. Phys. Lett. **79**, 2543 (2001).
[9] N.A. Clark and S.T. Lagerwall, Appl. Phys. Lett. **36**, 899 (1980).
[10] G. Andersson, I. Dahl, P. Keller, W. Kuczynski, S.T. Lagerwall, K. Skarp, and B. Stebler, Appl. Phys. Lett. **51**, 640 (1987).
[11] M.C. Mauguin, Bull. Soc. Fr. Mineral. Cristallogr. **34**, 71 (1911).
[12] S. Chandrasekhar, *Liquid Crystals* (Cambridge University Press, Cambridge, 1992).
[13] This situation for the effective helical pitch corresponds to $\varphi = \varphi_i$ at the interface and to $\varphi = 0$ at the center of the cell.
[14] T. Shioda, B. Wen, and C. Rosenblatt, Phys. Rev. E **67** 041706 (2003).
[15] The bulk liquid crystal also couples weakly ($\propto E^2$) to the electric field. This causes a very small increase in θ (*not* φ) throughout the cell, but having only dc and 2ω frequency components. Thus, coupling of the electric field to the bulk is observed in our experiment.
[16] B. Zeks, Mol. Cryst. Liq. Cryst. **114**, 259 (1984).
[17] P.K. Karahaliou, A.G. Vanakaras, and D.J. Photinos, Phys. Rev. E **65**, 031712 (2002).
[18] G.P. Sinha, C. Rosenblatt, and L.V. Mirantsev, Phys. Rev. E **65**, 041718 (2002).
[19] V.P. Vorflusev, H.S. Kitzerow, and V.G. Chigrinov, Jpn. J. Appl. Phys. Lett **34**, L1137 (1995).